Chlorococcum sp. MM11—a novel phyco-nanofactory for the synthesis of iron nanoparticles

ARTICLE *in* JOURNAL OF APPLIED PHYCOLOGY · JANUARY 2015

Impact Factor: 2.56 · DOI: 10.1007/s10811-014-0492-2

6 AUTHORS, INCLUDING:

Suresh ramraj Subashchandrabose
University of Newcastle
12 PUBLICATIONS **112** CITATIONS
SEE PROFILE

Thavamani Palanisami
University of Newcastle
45 PUBLICATIONS **190** CITATIONS
SEE PROFILE

Megharaj Mallavarapu
University of Newcastle
322 PUBLICATIONS **4,477** CITATIONS
SEE PROFILE

Ravi Naidu
University of South Australia
594 PUBLICATIONS **11,393** CITATIONS
SEE PROFILE

J Appl Phycol
DOI 10.1007/s10811-014-0492-2

Chlorococcum sp. MM11—a novel phyco-nanofactory for the synthesis of iron nanoparticles

Vidhyasri Subramaniyam · Suresh Ramraj Subashchandrabose · Palanisami Thavamani · Mallavarapu Megharaj · Zuliang Chen · Ravi Naidu

Received: 29 July 2014 / Revised and accepted: 1 December 2014

Abstract Green synthesis of iron nanoparticles using a soil microalga, *Chlorococcum* sp. MM11, and their application in chromium remediation have been investigated. Spherical-shaped nanoiron was synthesized by treating the exponentially growing culture of *Chlorococcum* sp. with 0.1 M iron chloride solution for 48 h and incubating it under shaking in the dark. The appearance of a yellowish brown colour indicated the biotransformation of bulk iron into nanoiron. Morphological characteristics of nanoparticles with transmission electron microscopy (TEM) and dynamic light scattering (DLS) confirmed the presence of spherical-shaped nanoiron ranging in size from 20 to 50 nm. TEM imaging also revealed the localization of nanoiron on the microalgal cell surface, inside as well as outside the cell. Fourier transform infrared spectroscopy (FTIR) analysis confirmed the involvement of carbonyl and amine bonds from polysaccharides and glycoproteins present in the algal cell wall in the bioreduction as well as capping of nanoiron. Phyco-synthesized iron nanoparticles were tested for their efficiency in reducing Cr(VI), a toxic environmental pollutant. The results showed that nanoiron reduced 92 % of 4 mg L^{-1} Cr(VI) to Cr(III) instantaneously, while bulk iron reduced only 25 %. Thus, iron nanoparticles with high reactivity, greater stability and environmentally benign and economically viable properties can be synthesized using phyco-nanofactories like *Chlorococcum* sp. MM11.

Keywords *Chlorococcum* sp · Chlorophyceae · Iron nanoparticle · Phyco-nanotechnology · Chromium reduction

Introduction

In recent years, much research has focussed on nanotechnology-based remediation for cleaning up environmental contaminants including Cr(VI). Cr(VI) is a highly soluble, mobile and toxic heavy metal contaminant that poses a serious threat to the environment. Additionally, iron nanoparticles are the most widely studied nanomaterial for the remediation of not only chromium but also other contaminants due to their high reducing properties, small size and high surface area (Zhang 2003). However, applying these engineered nanoparticles at field scale has some shortcomings. Firstly and primarily, the tendency of iron nanoparticles to agglomerate rapidly due to their high reactivity ultimately weakens the longevity of their reactivity and stability (Zhao and Xu 2007). Secondly, synthesis of nanoparticles by chemical methods involves utilizing precursor chemicals and toxic solvents and generating hazardous by-products which pose further threats to the environment. Therefore, it is essential to synthesize highly efficient nanoparticles in terms of their reactivity, stability, cost-effectiveness and environmental compatibility for the in situ remediation of contaminants.

In recent years, considerable research has been conducted on the biological synthesis of metal nanoparticles using bacteria, fungi, algae and plants (Mohanpuria et al. 2008; Thakkar et al. 2010). It is hypothesized that biomolecules such as flavonoids (Raghunandan et al. 2009), polyols (Begum et al. 2009), terpenoids (Shankar et al. 2004) and organic acids (Sharon et al. 2012) present in biological entities control the structure, phase, orientation and nanostructural topography of

Electronic supplementary material The online version of this article (doi:10.1007/s10811-014-0492-2) contains supplementary material, which is available to authorized users.

V. Subramaniyam (✉) · S. R. Subashchandrabose · P. Thavamani · M. Megharaj · Z. Chen · R. Naidu
Centre for Environmental Risk Assessment and Remediation, University of South Australia, Mawson Lakes Campus, Adelaide 5095, Australia
e-mail: subvy008@mymail.unisa.edu.au

V. Subramaniyam · S. R. Subashchandrabose · P. Thavamani · M. Megharaj · Z. Chen · R. Naidu
CRC for Contamination Assessment and Remediation of the Environment, Mawson Lakes, Adelaide 5095, Australia

Published online: 09 January 2015

inorganic crystals, resulting in nanosized particles (Ghashghaei and Emtiazi 2013). Examples of the carbonyl group such as aldehyde, ketone and carboxylic acid that are present in biomolecules actively reduce the metal salts to metals by donating electrons, thereby acting as reducing agents (Shankar et al. 2004). Moreover, several protein molecules were shown to bind with the metal through free amine groups or carboxylate ions (Gopinath et al. 2012). They increased their stability by preventing oxidation or agglomeration and thus acting as capping agents. Consequently, these nanoparticles are more stable, mobile and highly reactive than those synthesized by conventional chemical methods. Several studies reported the use of bioactive compounds from tea polyphenols (Nadagouda et al. 2010), sorghum bran extracts (Njagi et al. 2011) and *Pleurotus* sp. (Mazumdar and Haloi 2011) for the synthesis of iron nanoparticles. Recent studies have reported the successful application of iron nanoparticles on the biodegradation of anionic and cationic dyes (Shahwan et al. 2011) and bromothymol blue (Hoag et al. 2009).

Recently, synthesis of metal nanoparticles using algae has attracted much attention due to their simplicity and cost-effectiveness in terms of mass production as well as downstream processing of nanoparticles and environmental benignity; they greatly reduce the need for hazardous chemicals. Moreover, many algae have thick, rigid cell walls made up of polysaccharide and glycoprotein matrices containing several functional groups such as hydroxyl, carbonyl, carboxyl, thiol, sulfonate and amino and amidic groups (Kuyucak and Volesky 1989) which play a major role in metal reduction and accumulation. Additionally, several research studies proved the efficiency of algae in the remediation of toxic heavy metals by reducing them into non-toxic forms. Hence, the potentials of both micro- and macroalgae were experimentally confirmed for the synthesis of metal nanoparticles such as gold, silver, copper and palladium (Table 1) (Korbekandi and Iravani 2013). However, their effectiveness in the synthesis of iron nanoparticles as well as environmental application of these nanoparticles has not been successfully demonstrated. Indeed, to our knowledge, this is the first study that demonstrates the role of phyco-synthesized iron nanoparticles in heavy metal remediation.

In this study, we explored the ability of a soil alga, *Chlorococcum* sp., for the synthesis of iron nanoparticles as well as their application in remediation of toxic Cr(VI). The aims of the present study were the following: (i) phyco-synthesis of iron nanoparticles; (ii) characterization of iron nanoparticles using ultraviolet-visible spectrophotometry (UV-vis), transmission electron microscopy (TEM), energy-dispersive X-ray spectroscopy (EDAX) and Fourier transform infrared spectroscopy (FTIR) techniques; and (iii) assessing the efficiency of these iron nanoparticles in reducing chromium.

Materials and methods

Microalga Chlorococcum sp. MM11, originally isolated from soil and maintained axenically in the Phycology Laboratory at the Centre for Environmental Risk Assessment and Remediation, University of South Australia, was used for the study. Stock cultures were maintained in Bold's basal medium (BBM) under continuous light (200 μmol photons m^{-2} s^{-1} PFD) at 25±2 °C on an orbital shaker (Megharaj et al. 1986). Any contamination of the culture was checked periodically by

Table 1 Microalgae and macroalgae involved in metal nanoparticle synthesis

Algae	Nanoparticles	Size	Synthesis	Reference
Microalgae				
Chlorella vulgaris	Pd	2–15	Extracellular	Eroglu et al. 2013
Tetraselmis suecica	Au	79	–	Shakibaie et al. 2010
Chlorella vulgaris	Au	0.8–2 μm	–	Lee et al. 2007
Euglena gracilis	Fh	0.6–1.0	Intracellular	Brayner et al. 2012
Chlorella vulgaris	Au	12.62	Extracellular	Satapathy et al. 2014
Tetraselmis kochinensis	Au	5–35	Intracellular	Ahmad et al. 2012
Macroalgae				
Sargassum wightii	Au	8–12	Extracellular	Singaravelu et al. 2007
Rhizoclonium fontinale	Au	~16	–	Parial and Pal 2014
Bifurcaria bifurcata	CO	5–45	–	Abboud et al. 2014
Cystophora moniliformis	Ag	75	–	Prasad et al. 2013
Cyanobacteria				
Nostoc ellipsosporum	Au	435	Intracellular	Parial et al. 2012
Lyngbya majuscula, *Spirulina subsalsa* and *Rhizoclonium hieroglyphicum*	Au	<20	Intracellular	Chakraborty et al. 2009

streaking the culture on BBM medium and nutrient agar plates as well as by microscopic analysis.

Synthesis of iron nanoparticles *Chlorococcum* sp. MM11 was grown in BBM for 5 days under light on a shaker as described above. The exponentially growing cells were harvested by centrifugation at 4000×*g* for 10 min and washed three times with ultrapure water to remove any impurities in the medium. Then, 0.4 g (dry weight) of the alga was mixed with 5 mL of 0.1 M $FeCl_3$ (Sigma-Aldrich) solution and placed under dark conditions at 24 °C in an orbital shaker set at 120 rpm for 48 h. Similarly, 0.4 g alga incubated with 5 mL of ultrapure water under the same conditions served as a control. The aliquots were withdrawn periodically from the reaction mixture for characterization to confirm the presence of nanoiron.

Characterization of nanoparticles The samples were centrifuged at 4000×*g* for 5 min to remove the biomass from the reaction mixture. The supernatant containing iron nanoparticles was taken away for morphological and chemical characterization studies, while the biomass was subjected to FTIR and TEM analyses. Surface-volume ratio is an important criterion for assessing the nanotechnology's application. Surface-volume ratio depends on the size and shape of the particles. It is therefore necessary to characterize the synthesized nanoparticles according to their size and shape. The synthesized nanoparticles were subjected to chemical characterization in order to validate the chemical property of nanoiron and also to detect the involvement of biomolecules in reduction as well as capping.

UV-vis absorbance spectroscopy The spectra of algal extract, $FeCl_3$ solution and iron nanoparticle suspensions were obtained using a UV 3600 Shimadzu UV-VIS-NIR spectrophotometer by scanning between 200 and 550 nm to monitor the biotransformation. Due to their high optical density, the samples were diluted five times using double-distilled water to obtain unsurpassed absorbance data.

Particle size analysis The size of the synthesized nanoparticles was further estimated using a particle size analyzer (Nicomp-380ZLS/Accusizer-780). The sample including the iron nanoparticle suspension was diluted before analysis in order to obtain the best results. The polydispersity index (PDI) was calculated to understand the agglomeration of nanoparticles using the formula PDI=square of (standard deviation/mean diameter).

Transmission electron microscopy The morphology of the synthesized nanoiron was further confirmed by transmission electron microscopy. The samples were diluted ten times, and 5 μL of the sample was placed on a Formvar carbon-coated copper grid and then dried under vacuum. Following this, it was taken for TEM analysis in FEI Tecnai G2 Spirit TEM, which operated at an acceleration voltage of 200 kV. For whole cell analysis, the samples were fixed in a fixative containing 4 % paraformaldehyde, 1.25 % glutaraldehyde in PBS and 4 % sucrose at pH 7.2 and left overnight. Then, they were washed with washing buffer (phosphate-buffered saline+4 % sucrose) for 10 min. The washed sample was fixed in 2 % osmium tetroxide for 1 h and dehydrated in 70, 90 and 100 % ethanol (each repeated twice for 20 min) and propylene oxide for 10 min. The samples were then placed in a mixture containing propylene oxide and epoxy resin at the ratio of 1:1 for overnight, and this process was repeated with 100 % epoxy resin. Finally, the samples were embedded in fresh resin and polymerized in an oven at 70 °C for 24 h. TEM sections were obtained using a diamond knife, and they were then mounted on copper grids for imaging.

Energy-dispersive X-ray spectroscopy The EDAX spectra for the nanoparticles were obtained using FEI Tecnai G2 Spirit TEM equipped with an EDXA-detector to identify the elemental composition of the nanoparticles. Samples were prepared as shown in the transmission electron microscope section.

Fourier transform infrared spectroscopy FTIR analysis was done to confirm the involvement of biomolecules in the bioreduction process as well as capping. Chemical changes in the biomass after incubating with iron chloride solution assisted in determining the functional groups involved in the synthesis. The biomass following nanoparticle synthesis was harvested by centrifugation at 4000×*g* for 5 min, washed twice with ultrapure water to remove any impurities and dried for 30 min at 60 °C in a hot-air oven. Then, alga-KBr pellets were prepared by mixing, grinding and compressing 5 mg of alga with 200 mg of potassium bromide (KBr) (PIKE Technologies) in a CrushIR–digital hydraulic press. Infrared spectra of the control (biomass without iron) and the biomass involved in synthesis were obtained using the Agilent-Cary 660 Fourier transform infrared spectrometer system. The difference in the spectra yields information about the functional groups involved in the bioreduction and capping.

Cr(VI) reduction experiments The phyco-synthesized iron nanoparticles were tested for their efficiency in remediating Cr(VI). For this study, K_2CrO_4 (Sigma-Aldrich) was used as a Cr(VI) source. In order to find out the role of biomass and iron chloride on Cr(VI) reduction, biomass and iron chloride were used as controls. Moreover, $FeCl_3$ served as a reference control for this study. Equal volumes of $FeCl_3$ solution, biomass and iron nanoparticle suspension were treated with the artificial wastewater containing 4 mg L^{-1} of Cr(VI). Different concentrations of iron nanoparticles and Cr(VI) were treated to optimize and quantify the amount of nanoparticles required for the remediation of Cr(VI). The Cr(VI) concentrations were estimated spectrophotometrically using diphenyl carbazide

reagent (Nethaji et al. 2013). The percentage of Cr(VI) removal was calculated using the following formula:

$$\%\ \text{removal of Cr(VI)} = \left[C_{\text{initial}} - \frac{C_{\text{final}}}{C_{\text{initial}}}\right] \times 100$$

Results

The reddish yellow-coloured bulk iron chloride solution turned into a yellowish brown colour when treated with *Chlorococcum* sp. after 48 h of exposure in dark conditions. This could be due to the changes in plasmon resonance indicating the transformation of bulk iron into nanoiron. This is further confirmed in UV-vis by scanning the absorbance profile of bulk iron chloride solution, biomass solution and nanoiron suspension. It indicated the presence of an iron peak around 293 nm in bulk iron as well as in nanoiron, while at the same time, it was lacking in biomass control solution. However, a shift occurred in the absorption peak in the nanoiron suspension compared to the bulk iron (Fig. 1). This shift in the peak is due to changes in the size as well as intensity of particles present in the medium.

Size distribution and intensity of nanoparticles in bulk iron and nanoiron suspension were analysed in the particle size analyser using dynamic light scattering (DLS). DLS analysis revealed the presence of iron nanoparticles with the size ranging from 20 to 50 nm and an average diameter of 35.8 nm. Also, the volume by weight of nanoparticles in the suspension was found to have a fit error of 29.43 (Fig. 2). Moreover, the polydispersity index was found to be 0.01 which is less than 0.1, indicating the monodispersity of iron nanoparticles.

The size of the nanoiron as well as biomolecule capping was further confirmed microscopically by TEM examination. TEM images confirmed the presence of 20–50 nm sized nanoparticles spherical in shape (Fig. 3a, b). Moreover, the attachment of biomolecules to nanoiron is clearly documented in Fig. 3b. Apart from dense localization of nanoiron on the outer membrane of *Chlorococcum* sp., Fig. 3c also shows the intra- and extracellular punctuated localization of nanoiron. This further confirmed that nanoparticle synthesis occurred such as adhesion of bulk iron on the cell surface, reduction of bulk iron into nanoiron on the cell surface and release of nanoiron outside the cell or uptake by the cell.

It is evident from the EDAX spectra that the spherical-shaped nanoparticles were iron as indicated by the iron peak (Fig. 4), not iron oxide, as the intensity of the oxygen peak is comparatively lower. Moreover, the presence of oxygen as well as carbon peak in the spectra could be from biomolecules, indicating the involvement of biomolecules in capping the nanoiron. On the other hand, the copper peak obtained was derived from the copper grid used to load the samples for the analysis. Although a chloride peak is present in the spectra, it is of very low intensity, while the 1:1 atomic percentage ratio of iron and chloride (data not shown) indicated the reduction of iron chloride to nanoiron.

The FTIR spectra for the algal biomass showed a distinguished peak at 3256, 3058 cm^{-1} which corresponds to the O–H group of polysaccharides. The absorption peak observed at 2912, 2842 cm^{-1} indicated the presence of the C–H stretching band of alkanes. However, the IR peak between 2354 and 2320 cm^{-1} corresponds to CO_2. Furthermore, the absorption peak observed between 1200 and 1700 cm^{-1} corresponds to protein that has three distinguished amide bands, these being amide I (1600–1690 cm^{-1}), amide II (1480–1575 cm^{-1}) and amide III (1229–1301 cm^{-1}). However, the IR vibrational peak obtained between 1200 and 800 cm^{-1} indicated the presence of carbohydrates. Moreover, the absorption peaks

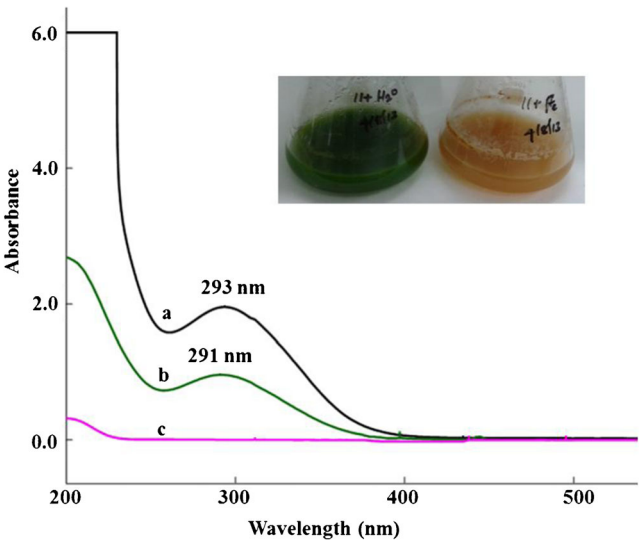

Fig. 1 UV-vis spectra of *a* bulk iron, *b* nanoiron, and *c* biomass showing surface plasmon resonance band at 293 nm for bulk iron and 291 nm for nanoiron. *Inset picture* showing the appearance of a *yellowish black* colour after the synthesis of nanoiron

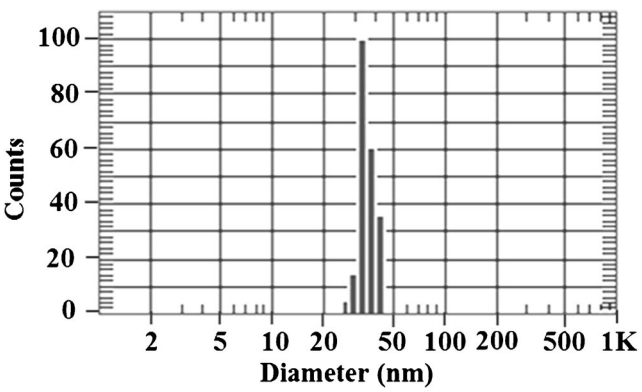

Fig. 2 Size of the nanoiron by DLS study in the particle size analyser

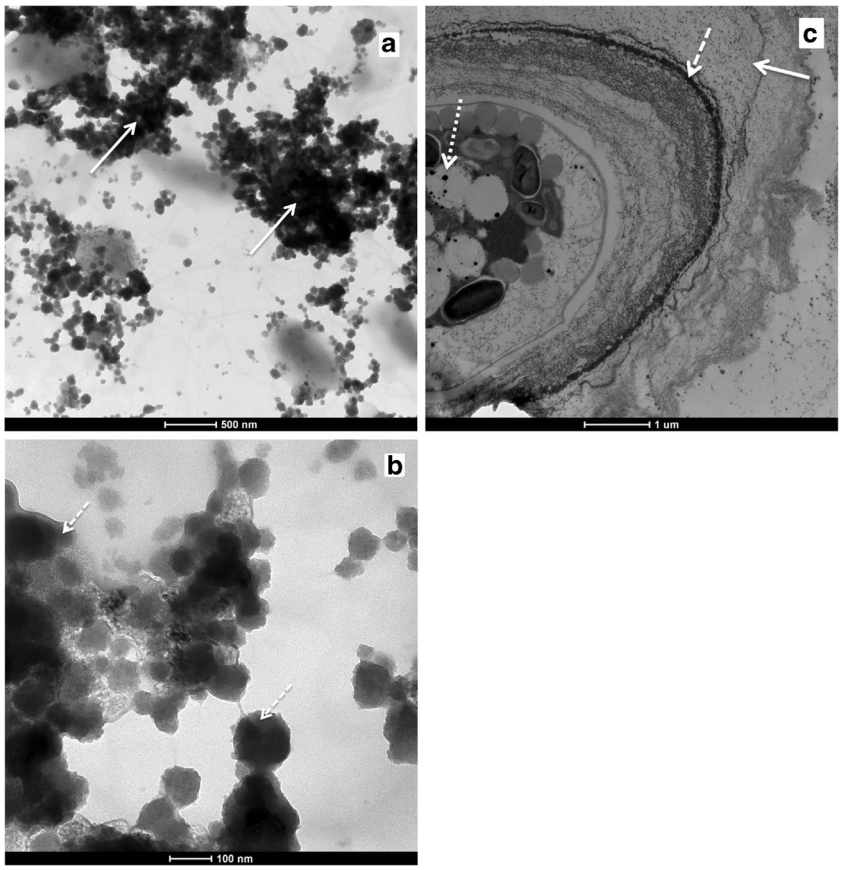

Fig. 3 TEM images of phyco-synthesized iron nanoparticle; **a** presence of nanoiron outside the cell (*solid arrows*), **b** capping of nanoiron by biomolecules (*dashed arrows*), **c** localization of nanoiron on the cell surface (*dashed arrows*), inside (*dashed arrows*) and outside (*solid arrows*) the cell

for the C–O, C=O, O–H, C–H, C–N and N–H bonds in the functional groups of carbohydrates and proteins are illustrated in supplementary material I. In order to indicate the involvement of functional groups in bioreduction, the IR spectra of algal biomass after nanoparticle synthesis were compared with the control (biomass without iron treatment) (Fig. 5). Remarkably, there was an intense broad absorption spectrum for C–H and O–H bonds at 2912, 2842 and 3256, 3058 cm^{-1}, respectively. This may be due to the hydrolysis of carbohydrates. On the other hand, the absorption peak intensity at 1757 cm^{-1} corresponds to the carbonyl group, while the 1492 absorption peak corresponding to the N–H group decreased. It is clearly evident from the FTIR spectra that changes in the functional groups corresponding to carbohydrates and proteins confirmed their involvement in bioreduction and the capping process.

The phyco-synthesized nanoiron has the ability to reduce Cr(VI) to Cr(III) instantaneously. The results showed that nanoiron reduced 92 % of 4 mg L^{-1} Cr(VI) compared to bulk iron (25 %) while the biomass control indicated no reduction (Fig. 6). This confirmed that the synthesized nanoparticles were actively involved in reducing Cr(VI). Moreover, the results also proved that nanoiron was more efficient in removing Cr(VI) than bulk iron. Considering the optimization experiments, the results indicated a clear dose-response relationship. An increase in chromium concentration decreased the percentage of Cr(VI) removed whereas an increase in nanoparticle concentration increased the Cr(VI) removal percentage

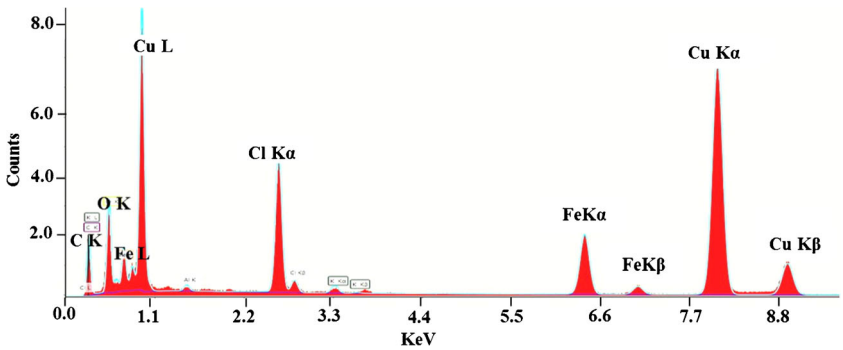

Fig. 4 EDAX spectrum of phyco-synthesized iron nanoparticle showing absorption peaks for Fe, C, O, Cu and Cl

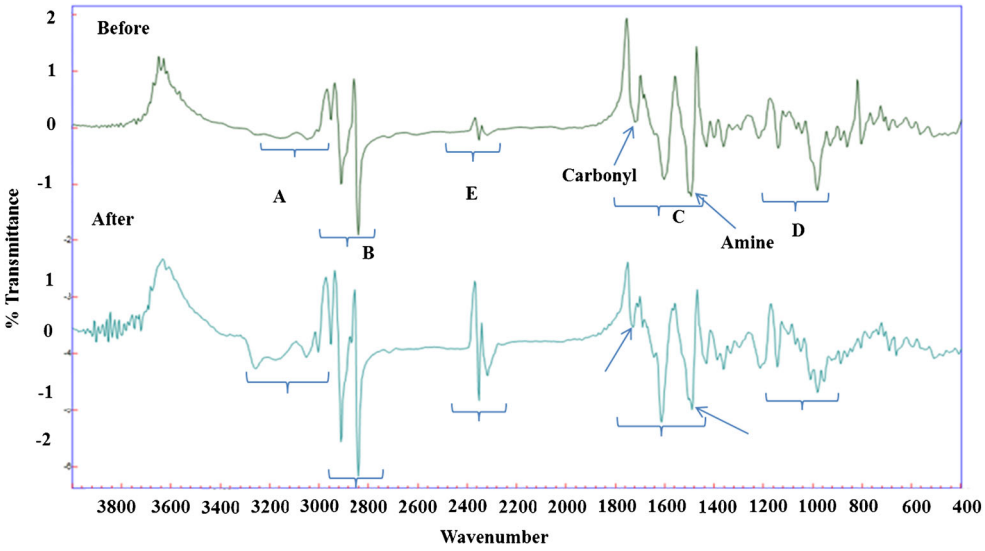

Fig. 5 FTIR spectra of biomass obtained before and after the nanoparticle synthesis; *arrows* indicate the carbonyl bond and amine bond in the treated biomass. *A* O–H bond; *B* C–H bond; *C* protein peaks; *D* carbohydrate peaks; *E* CO_2 peak (for further information related to FTIR spectra, refer to Table S1 in supporting document)

(Fig. 7a, b). From the optimization studies, it was observed that a minimum of 0.5 mL (2 μg L^{-1}) of iron nanoparticle suspension was required to reduce 4 mg L^{-1} of Cr(VI).

Discussion

Recently, Korbekandi and Iravani (2013) reported that the biomolecules present in algae are able to reduce metal ions to metal nanoparticles. In this study, iron nanoparticles were produced by incubating *Chlorococcum* sp., harvested at exponential phase with bulk iron chloride solution for 48 h under dark conditions. An earlier study showed that algal extracts could be used to synthesize metal nanoparticles (Shakibaie et al. 2010). The formation of a yellowish black colour is due to surface plasmon vibration of electrons from nanoiron, which indicates the transformation of bulk iron into nanoiron.

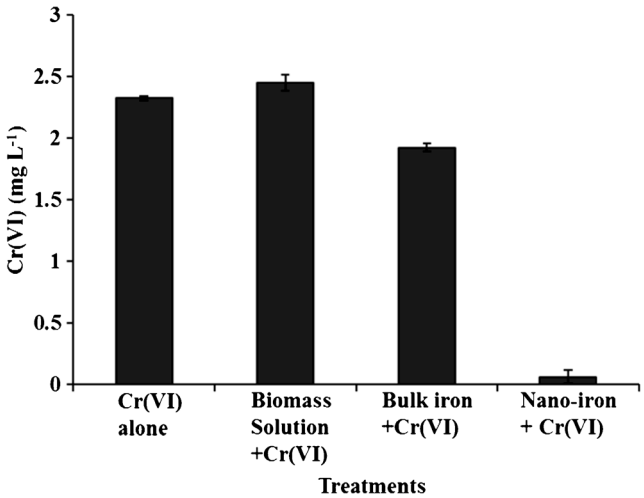

Fig. 6 Reduction of Cr(VI) by $FeCl_3$ solution, iron nanoparticles and biomass (*error bar* indicates standard deviation, n=3)

This surface plasmon vibration of electrons varies with different sizes and shapes of nanoparticles. However, shifting of the peak towards the lower wavelength clearly indicates the presence of small-sized iron nanoparticles (kebede et al. 2013). In contrast, shifting of the peak towards the longer wavelength indicates the presence of larger-sized nanoparticles. In this study, the surface plasmon resonance in aqueous medium for

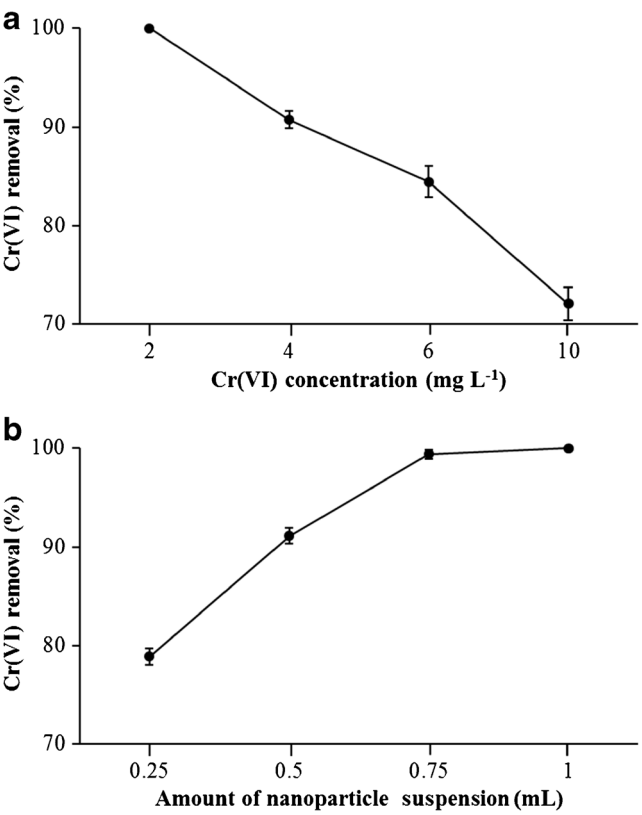

Fig. 7 Effect of **a** Cr(VI) concentration and **b** nanoparticle concentration on chromium reduction by phyco-synthesized iron nanoparticle (*error bar* indicates standard deviation, n=3)

nanoiron occurs at 291 nm which is 2 nm lesser than the bulk iron. Although shifting is only small, it does not directly correlate with the size of the nanoparticle, as the capping by the biomolecules always enhance the size of the synthesized particles (Mohan Kumar et al. 2013). Consistent with this, the DLS study proved that the nanoparticles' size in the present study ranges from 20 to 50 nm and the TEM image confirmed the capping of nanoiron by biomolecules.

Earlier studies concluded that nanoparticles with well-defined size and shape can be achieved by adjusting reaction parameters such as growth phase (Sweeney et al. 2004), cell-extract concentration (Wei et al. 2012; Parial and Pal 2014), metal ion concentration (Juibari et al. 2011; Parial and Pal 2014), pH (Sinha and Khare 2011; Parial and Pal 2014), temperature (Juibari et al. 2011) and incubation time (Sinha and Khare 2011). Evidently, Nadagouda et al. (2010) also reported that the production of iron nanoparticles having different shapes such as spherical, platelets, irregular and nanorods was possible by altering the ratio of reactants such as tea extract and $Fe(NO_3)_3$. However, in this study, the hypothesized spherical-shaped iron nanoparticles ranging in size from 20 to 50 nm were produced by the microalgae without involving the above factors. This could be due to the role played by live algal cells supplying the required amount of biomolecules for reducing given metal ion solutions compared to algal extracts, other microbes and plant extracts. This is consistent with the statement that microorganisms produce nanoparticles with good monodispersity and well-defined morphologies compared to plant extracts.

The FTIR spectra of treated and untreated algal biomass revealed the involvement of carbohydrates and proteins in bioreduction and capping. Decreased intensity of the carbonyl group in the treated biomass suggests that the negatively charged carbonyl group attracted the positively charged metal ions and reduced them to metal nanoparticles by donating the electrons. The carbonyl bond is attributed to the functional group such as carboxylic acid, aldehydes and ketones present in the polysaccharides of the algal cell wall. This is further confirmed by the increased intensity of hydroxyl groups which may be due to the hydrolysis of carbohydrates (Han et al. 2007). Similarly, Shankar et al. (2004) reported that the carbonyl bond present in the functional group of *Azadirachta indica* biomolecules reduced gold and silver metal ions to Au-Ag bimetallic nanoparticles. Additionally, the decreased intensity of the amine group indicates the possibility of synthesized nanoparticles binding to the free amine group (Gopinath et al. 2012). The amine bond is attributed to the amino acid functional group present in the glycoprotein of the algal cell wall, enzymes and other proteinaceous substances. This means that polysaccharides and glycoproteins present in the algal cell wall are involved in bioreduction and capping. Confirming this statement, the TEM image of the whole cell after nanoparticles were synthesized showed the nanoparticles being localized on the outer cell wall of the alga. Thus, the involvement of the cell wall in the bioreduction process is indicated. The overall mechanism for the bioreduction of bulk iron to nanoiron is illustrated below. However, further studies are required to prove this proposed mechanism.

Mechanism involved in the phyco-synthesis of nanoiron

Step 1: Reduction of the iron ion by the carbonyl group into an iron nanoparticle

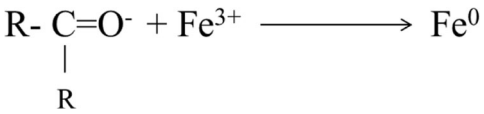

Step 2: Binding of nano-Fe to the amine bond

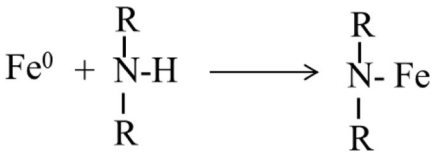

In this study, application of phyco-synthesized iron nanoparticles in the remediation of Cr(VI) was successfully achieved. The nanoiron reduced 92 % of Cr(VI) while bulk

Table 2 Comparison between iron nanoparticles produced from different sources

Synthesis		Characters				Reference
		Size (nm)	Stability	Nanoparticles	Cr(VI)	
Chemical	Montmorillonite Fe-Ni	20–40	–	0.8 g L^{-1}	10 mg L^{-1}	Kadu et al. 2011
	CMC stabilized	20–100	>15 days	0.15 g L^{-1}	10 mg L^{-1}	Wang et al. 2010
Biological	Plant synthesized	50–80	2 months	20 μg L^{-1}	10 mg L^{-1}	Madhavi et al. 2013
	Phyco-synthesized	20–50	3 months[a]	5 μg L^{-1}	10 mg L^{-1}	Present work

[a] Data not shown

iron reduced only 25 %. The higher efficiency of nanoiron is due to a higher surface area for the reduction of contaminants compared to bulk iron. Thus, 2 μg L^{-1} of nanoiron is more than sufficient to reduce 4 mg L^{-1} of Cr(VI) concentration. This is consistent with the efficiency of iron nanoparticles produced by *Eucalyptus globulus* in removing Cr(VI) (Madhavi et al. 2013). Nonetheless, the remediation of Cr(VI) requires larger amounts of carboxy methyl cellulose (CMC)-stabilized nanoparticles and montmorillonite Fe-Ni nanoparticles than phyco-synthesized nanoparticles (Table 2). This could be explained by the greater stability as well as size of iron nanoparticles and greater surface area for Cr(VI) reduction by phyco-synthesized iron nanoparticles.

To conclude, this investigation demonstrated the following: firstly, the potential of *Chlorococcum* sp. in a fairly monodispersed iron nanoparticle synthesis, and secondly, applying phyco-synthesized nanoiron for the remediation of Cr(VI). Biomolecules such as polysaccharides and glycoprotein present in the algal cell wall acted as reducing and capping agents for nanoiron. Moreover, nanoparticles with key properties such as greater reactivity, abundant extended activity and low toxicity were achieved effectively at low cost. This technology is efficient in removing contaminants, suggesting that green-based phyco-nanotechnology has great potential as an alternative to chemical-based approaches.

Acknowledgments The VS acknowledge Endeavour Awards and CRC-CARE for providing Scholarship, University of South Australia for the research facilities and University of Adelaide for Transmission Electron Microscope analysis.

References

Abboud Y, Saffaj T, Chagraoui A, El Bouari A, Brouzi K, Tanane O, Ihssane B (2014) Biosynthesis, characterization and antimicrobial activity of copper oxide nanoparticles (CONPs) produced using brown alga extract (*Bifurcaria bifurcata*). Appl Nanosci 4: 571–576

Ahmad A, Senapati S, Syed A, Moeez S, Kumar A (2012) Intracellular synthesis of gold nanoparticles using alga *Tetraselmis kochinensis*. Mater Lett 79:116–118

Begum NA, Mondal S, Basu S, Laskar RA, Mandal D (2009) Biogenic synthesis of Au and Ag nanoparticles using aqueous solutions of black tea leaf extracts. Colloid Surf B 71:113–118

Brayner R, Coradin T, Beaunier P, Grenèche JM, Djediat C, Yéprémian C, Couté A, Fiévet F (2012) Intracellular biosynthesis of superparamagnetic 2-lines ferri-hydrite nanoparticles using *Euglena gracilis* microalgae. Colloid Surf B 93:20–23

Chakraborty N, Banerjee A, Lahiri S, Panda A, Ghosh AN, Pal R (2009) Biorecovery of gold using cyanobacteria and an eukaryotic alga with special reference to nanogold formation—a novel phenomenon. J Appl Phycol 21:145–152

Eroglu E, Chen X, Bradshaw M, Agarwal V, Zou J, Stewart SG, Duan X, Lamb RN, Smith SM, Raston CL, Iyer SK (2013) Biogenic production of palladium nanocrystals using microalgae and their immobilization on chitosan nanofibers for catalytic applications. RSC Adv 3:1009–1012

Ghashghaei S, Emtiazi G (2013) Production of hydroxyapatite nanoparticles using tricalcium-phosphate by *Alkanindiges illinoisensis*. J Nanomater Mol Nanotechnol 2:5

Gopinath V, Ali MD, Priyadarshini S, Priyadharsshini NM, Thajuddin N, Velusamy P (2012) Biosynthesis of silver nanoparticles from *Tribulus terrestris* and its antimicrobial activity: a novel biological approach. Colloid Surf B 96:69–74

Han X, Wong YS, Wong MH, Tam NFY (2007) Biosorption and bioreduction of Cr(VI) by a microalgal isolate, *Chlorella miniata*. J Hazard Mater 146:65–72

Hoag GE, Collins JB, Holcomb JL, Hoag JR, Nadagouda MN, Varma RS (2009) Degradation of bromothymol blue by 'greener' nano-scale zero-valent iron synthesized using tea polyphenols. J Mater Chem 19:8671–8677

Juibari MM, Abbasalizadeh S, Jouzani GS, Noruzi M (2011) Intensified biosynthesis of silver nanoparticles using a native extremophilic *Ureibacillus thermosphaericus* strain. Mater Lett 65:1014–1017

Kadu BS, Sathe YD, Ingle AB, Chikate RC, Patil KR, Rode CV (2011) Efficiency and recycling capability of montmorillonite supported Fe–Ni bimetallic nanocomposites towards hexavalent chromium remediation. Appl Catal B Environ 104:407–414

Kebede A, Singh AK, Rai PK, Giri NK, Rai AK, Watal G, Gholap AV (2013) Controlled synthesis, characterization, and application of iron oxide nanoparticles for oral delivery of insulin. Lasers Med Sci 28:579–587

Korbekandi H, Iravani S (2013) Biological synthesis of nanoparticles using algae. Berforts Information Press Limited, UK, 53 pp

Kuyucak N, Volesky B (1989) The mechanism of cobalt biosorption. Biotechnol Bioeng 33:823–831

Lee JH, Han J, Choi H, Hur HG (2007) Effects of temperature and dissolved oxygen on Se(IV) removal and Se(0) precipitation by *Shewanella* sp. HN-41. Chemosphere 68:1898–1905

Madhavi V, Prasad T, Reddy AVB, Reddy RB, Madhavi G (2013) Application of phytogenic zerovalent iron nanoparticles in the adsorption of hexavalent chromium. Spectrochim Acta A 116:17–25

Mazumdar H, Haloi N (2011) A study on biosynthesis of iron nanoparticles by *Pleurotus* sp. J Microbiol Biotech Res 1:39–49

Megharaj M, Venkateswarlu K, Rao A (1986) Growth response of four species of soil algae to monocrotophos and quinalphos. Environ Pollut A 42:15–22

Mohan Kumar K, Mandal BK, Kumar SK, Reddy SP, Sreedhar B (2013) Biobased green method to synthesise palladium and iron nanoparticles using *Terminalia chebula* aqueous extract. Spectrochim Acta A 102:128–133

Mohanpuria P, Rana NK, Yadav SK (2008) Biosynthesis of nanoparticles: technological concepts and future applications. J Nanoparticle Res 10:507–517

Nadagouda MN, Castle AB, Murdock RC, Hussain SM, Varma RS (2010) *In vitro* biocompatibility of nanoscale zerovalent iron particles (NZVI) synthesized using tea polyphenols. Green Chem 12: 114–122

Nethaji S, Sivasamy A, Mandal A (2013) Preparation and characterization of corn cob activated carbon coated with nanosized magnetite particles for the removal of Cr(VI). Bioresour Technol 134:94–100

Njagi EC, Huang H, Stafford L, Genuino H, Galindo HM, Collins JB, Hoag GE, Suib SL (2011) Biosynthesis of iron and silver nanoparticles at room temperature using aqueous Sorghum bran extracts. Langmuir 27:264–271

Parial D, Pal R (2014) Biosynthesis of monodisperse gold nanoparticles by green alga *Rhizoclonium* and associated biochemical changes. J Appl Phycol. doi:10.1007/s10811-014-0355-x

Parial D, Patra HK, Roychoudhury P, Dasgupta AK, Pal R (2012) Gold nanorod production by cyanobacteria—a green chemistry approach. J Appl Phycol 24:55–60

Prasad TN, Kambala VSR, Naidu R (2013) Phyconanotechnology: synthesis of silver nanoparticles using brown marine algae *Cystophora moniliformis* and their characterisation. J Appl Phycol 25:177–182

Raghunandan D, Basavaraja S, Mahesh B, Balaji S, Manjunath S, Venkataraman A (2009) Biosynthesis of stable polyshaped gold nanoparticles from microwave-exposed aqueous extracellular anti-malignant guava (*Psidium guajava*) leaf extract. Nanobiotechnology 5:34–41

Satapathy S, Shukla SP, Sandeep KP, Singh AR, Sharma N (2014) Evaluation of the performance of an algal bioreactor for silver nanoparticle production. J Appl Phycol. doi:10.1007/s10811-014-0311-9

Shahwan T, Sirriah AS, Nairat M, Boyac IE, Eroglu A, Scott T, Hallam K (2011) Green synthesis of iron nanoparticles and their application as a Fenton-like catalyst for the degradation of aqueous cationic and anionic dyes. Chem Eng J 172:258–266

Shakibaie M, Forootanfar H, Mollazadeh-Moghaddam K, Bagherzadeh Z, Nafissi-Varcheh N, Shahverdi AR, Faramarzi MA (2010) Green synthesis of gold nanoparticles by the marine microalga *Tetraselmis suecica*. Biotechnol Appl Biochem 57:71–75

Shankar SS, Rai A, Ahmad A, Sastry M (2004) Rapid synthesis of Au, Ag and bimetallic Au core–Ag shell nanoparticles using Neem (*Azadirachta indica*) leaf broth. J Colloid Interface Sci 275:496–502

Sharon M, Pandey S, Oza G, Vishwanathan M (2012) Biosynthesis of highly stable gold nanoparticles using *Citrus limone*. Ann Biol Res 3:2378–2382

Singaravelu G, Arockiamary JS, Kumar VG, Govindaraju K (2007) A novel extracellular synthesis of monodisperse gold nanoparticles using marine alga, *Sargassum wightii* Greville. Colloid Surface B 57:97–101

Sinha A, Khare SK (2011) Mercury bioaccumulation and simultaneous nanoparticle synthesis by *Enterobacter* sp. cells. Bioresour Technol 102:4281–4284

Sweeney RY, Mao C, Gao X, Burt JL, Belcher AM, Georgiou G, Iverson BL (2004) Bacterial biosynthesis of cadmium sulfide nanocrystals. Chem Biol 11:1553–1559

Thakkar KN, Mhatre SS, Parikh RY (2010) Biological synthesis of metallic nanoparticles. Nanomed Nanotechnol 6:257–262

Wang Q, Qian H, Yang Y, Zhang Z, Naman C, Xu X (2010) Reduction of hexavalent chromium by carboxymethyl cellulose-stabilized zero-valent iron nanoparticles. J Contam Hydrol 114:35–42

Wei X, Luo M, Li W, Yang L, Liang X, Xu L, Kong P, Liu H (2012) Synthesis of silver nanoparticles by solar irradiation of cell-free *Bacillus amyloliquefaciens* extracts and $AgNO_3$. Bioresour Technol 103:273–278

Zhang W (2003) Nanoscale iron particles for environmental remediation: an overview. J Nanoparticle Res 5:323–332

Zhao D, Xu Y (2007) Reductive immobilization of chromate in water and soil using stabilized iron nanoparticles. Water Res 41:2101–2108